4. SIMPLIFIED MODEL ANALYSIS

4.1 INTRODUCTION

In this chapter, two simplified models are presented to replace the complex 3D finite element model by a relatively simple 2D approximation. These two simplified models can save the rigorous efforts and computer costs required for the analysis of a double angle connection.

The first model will be referred to as the simplified angle model. This simplified angle model is introduced to simulate the behavior of the outstanding leg of an angle. The simplified angle model is basically a beam in double curvature. Since the major behavioral characteristic of a double angle connection is the bending of the outstanding leg in the elastic range (Stefano and Astaneh, 1991, and Thornton, 1997), the beam can be used as an appropriate substitution for this angle behavior. From this simplified angle model, the initial axial stiffness of a connection can be easily determined.

The second model is the equivalent spring model. This equivalent spring model is suggested to establish the behavior of the angle behavior more easily by introducing two springs. A translational spring and a rotational spring are used to simulate the behavior of an angle under axial tensile loads and shear loads, respectively. The stiffness of each spring can be obtained from the regression curves of the 3D finite element model by using Richard’s formula.

4.2 SIMPLIFIED ANGLE MODEL

In the development of this simplified angle model, the center of the bolt fastened to the column flange is assumed to be a fixed support, while the center of the back-to-back angle leg is assumed to be a movable fixed end. The applied tensile load is assumed to act at the movable end. Figure 4.1 shows the simplified angle model and its cross section.

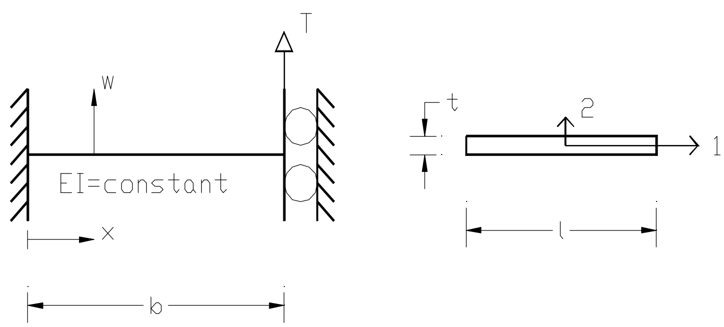

Figure 4.1 Simplified Angle Model

The equilibrium equation and general solution of this simplified angle model are

$$
\begin{aligned}
&EIw''''(x) = 0, \\
&w(x) = A_1 + A_2 x + A_3 x^2 + A_4 x^3
\end{aligned}
\tag{4.1}
$$

The boundary conditions of the simplified angle model are:

At the fixed end (x=0),

$$
\begin{aligned}
&w(0) = 0, \\
&w'(0) = 0
\end{aligned}
\tag{4.2}
$$

At the movable end (x=*b*),

$$
\begin{aligned}
&w'(b) = 0, \\
&EIw'''(b) = -T
\end{aligned}
\tag{4.3}
$$

By applying the above boundary conditions, the solution can be obtained with coefficients as follows:

$$A_1 = 0,$$
$$A_2 = 0,$$
$$A_3 = \frac{Tb}{4EI}, \qquad (4.4)$$
$$A_4 = -\frac{T}{6EI}$$

where,

t = angle thickness

l = length of the angle

I = moment of inertia of the angle

$= \frac{lt^3}{12}$

Then,

$$w(x) = (\frac{Tb}{4EI})x^2 - (\frac{T}{6EI})x^3 \qquad (4.5)$$

The initial stiffness for the simplified angle model can be obtained by introducing the given data into Equation 4.5 as follows:

$$K_{ini.} = \frac{T}{w(b)} = El(\frac{t}{b})^3 \qquad (4.6)$$

For the L5x3x1/4 angle specimen, the initial stiffness is calculated with given geometric properties using Equation 4.6 as follows:

$$K_{ini.} = El(\frac{t}{b})^3 = (29000)(11.5)(\frac{0.25}{3.475})^3 = 124.2\,kips/in. \qquad (4.7)$$

Similarly, for the L5x3x3/8 angle,

$$K_{ini.} = El(\frac{t}{b})^3 = (29000)(11.5)(\frac{0.375}{3.4125})^3 = 442.6\, kips / in. \qquad (4.8)$$

and for the L5x3x1/2 angle,

$$K_{ini.} = El(\frac{t}{b})^3 = (29000)(11.5)(\frac{0.5}{3.35})^3 = 1108.9\, kips / in. \qquad (4.9)$$

This initial stiffness for each angle specimen is compared to that from the 3D nonlinear finite element anaysis in Table 4.1.

Table 4.1 Comparison of Initial Stiffness of Each Angle

	3D Finite Element Model (kips/in.)	Simplified Angle Model (kips/in.)	% Difference
L5X3X1/4 Angle	116.7	124.2	6.4
L5X3X3/8 Angle	477.5	442.6	7.3
L5X3X1/2 Angle	1012.6	1108.9	9.5

4.3 EQUIVALENT SPRING MODEL

Two springs are attached to one end of a simply supported beam in this equivalent spring model. The axial tensile load, *T*, is applied to the other end of the beam, while the uniformly distributed load, *Q*, is applied to the top of the beam as shown in Figure 4.2.

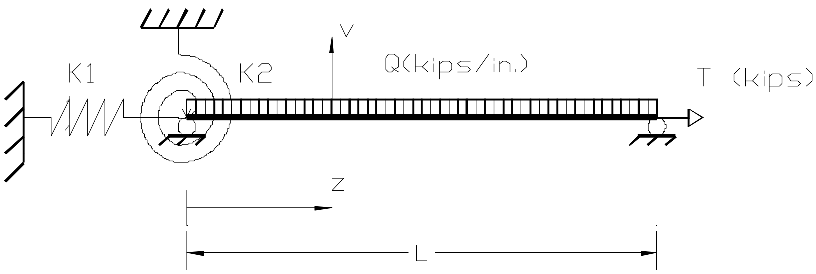

Figure 4.2 Equivalent Spring Model

The equilibrium equation and general solution of this equivalent spring model in the elastic region are

$$EIv''''(z) - Tv''(z) = -Q,$$
$$v(z) = A_1 e^{gz} + A_2 e^{-gz} + A_3 z + A_4 + \frac{Q}{2T} z^2 \qquad (4.10)$$

where,

$$g = \sqrt{\frac{T}{EI}}$$

I = moment of inertia of the beam (4.11)

The boundary conditions of the simplified double angle connection model are:

At z = 0,

$$v(0) = 0,$$
$$EIv''(0) - K_2 v'(0) = 0 \qquad (4.12)$$

At z = L,

$$v(L) = 0,$$
$$EIv''(L) = 0 \tag{4.13}$$

By applying the boundary conditions, the solution is written as follows:

$$v(z) = R_7 e^{\gamma z} + R_8 e^{-\gamma z} + R_9 z + R_{10} + \frac{Q}{2T} z^2 \tag{4.14}$$

where,

$$R_1 = EI\gamma^2 - K_2\gamma - EI\gamma^2 e^{2\gamma L} - e^{2\gamma L}\gamma K_2,$$
$$R_2 = \frac{Q}{\gamma^2} - \frac{Qe^{\gamma L} EI}{T} - \frac{Qe^{\gamma L} K_2}{\gamma T},$$
$$R_3 = \frac{R_1}{K_2},$$
$$R_4 = \frac{R_2}{K_2},$$
$$R_5 = e^{2\gamma L} - 1,$$
$$R_6 = \frac{Q}{\gamma^2 T e^{-\gamma L}},$$
$$R_7 = \frac{1}{R_3 L + R_5}\left(\frac{Q}{\gamma^2 T} - R_4 L - R_6 - \frac{Q}{2T} L^2\right),$$
$$R_8 = -e^{2\gamma L} R_7 - \frac{Q}{\gamma^2 T e^{-\gamma L}},$$
$$R_9 = R_3 R_7 + R_4,$$
$$R_{10} = R_5 R_7 + R_6 \tag{4.15}$$

K_1 = translational spring stiffness

K_2 = rotational spring stiffness

L = length of the beam

The angle change, θ, at z=0 is obtained from the first derivative of Equation 4.14 as follows:

$$\theta = v'(0) = R_7\gamma - R_8\gamma + R_9 \tag{4.16}$$

The relationship between the uniformly distributed load, Q, and the angle change, q, at z=0 is obtained for a given rotational spring stiffness, K_2, by using Equation 4.15 and Equation 4.16.

Figure 4.3 shows the uniformly distributed load-rotation relationship of a double angle connections with given rotational spring stiffnesses, K_2, of 5,700 in.-kips/rad., 20,750 in.-kips/rad., and 50,380 in.-kips/rad, which correspond to L5x3x1/4, L5x3x3/8, and L5x3x1/2 angles, respectively. These rotational spring stiffnesses are obtained from the regression curves of the 3D finite element model by using Richard's formula. When the uniformly distributed load, Q, is 0.3 kips/in., the rotational angle change, q, is 0.022 rad. for the given rotational spring stiffness of 5,700 in.-kips/rad. For the given rotational spring stiffness of 20,750 in.-kips/rad., the rotational angle change, q, is 0.019 rad. with the same uniformly distributed loading condition. Similarly, the rotational angle change, q, is 0.015 rad. with the given rotational spring stiffness of 50,380 in.-kips/rad.

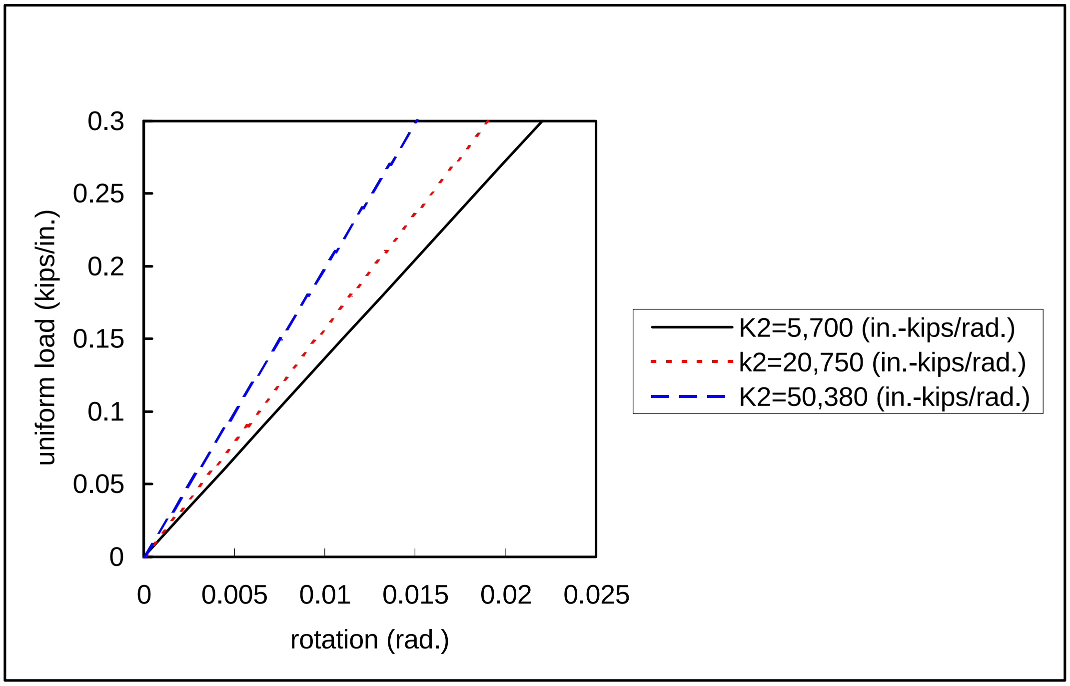

Figure 4.3 Uniformly Distributed Load vs. Rotation Relationship

4.3.1 Equivalent Spring Model Under Axial Tensile Loading

Since the above solution is only valid for the linearly elastic range, ABAQUS is used to investigate the equivalent spring model in the full range. The B33 (2-node cubic beam) element type and the SPRING2 (spring between two nodes, acting in a fixed direction) element type are chosen for the equivalent spring model to establish the load-displacement relationship of a double angle connection under axial tensile loading. The same model shown in Figure 4.2 is used for the ABAQUS executions. The load-displacement relationship can be obtained by determining the variation of the axial displacement of the beam at z=0 with the applied tensile load. Like the 3D finite element executions, the execution of the equivalent spring model is terminated when the displacement of the beam at z=0 exceeds 0.5 in. The translational spring stiffness, K_1, can be obtained from a regression analysis of the load-displacement curve of the 3D finite element model. Figure 4.4 shows the load-displacement curves of the L5x3x1/4 double angle connection. The 3D FEM curve is in Figure 2.6 and the equivalent spring model is based on the Richard's formula parameters in Table 2.10. The axial tensile load, *T*, varies from 0 kips to approximately 12 kips for this case. The axial tensile load, *T*, is applied to one end of the beam in the positive Z-direction. The load-displacement curve for the equivalent spring model shows good agreement with that of the 3D finite element model from the beginning of the loading. The initial stiffness of the equivalent spring model is 144.9 kips/in., while that of the 3D finite element model is 116.7 kips/in. Table 4.2 contains the data for the load-displacement relationship of the equivalent spring model.

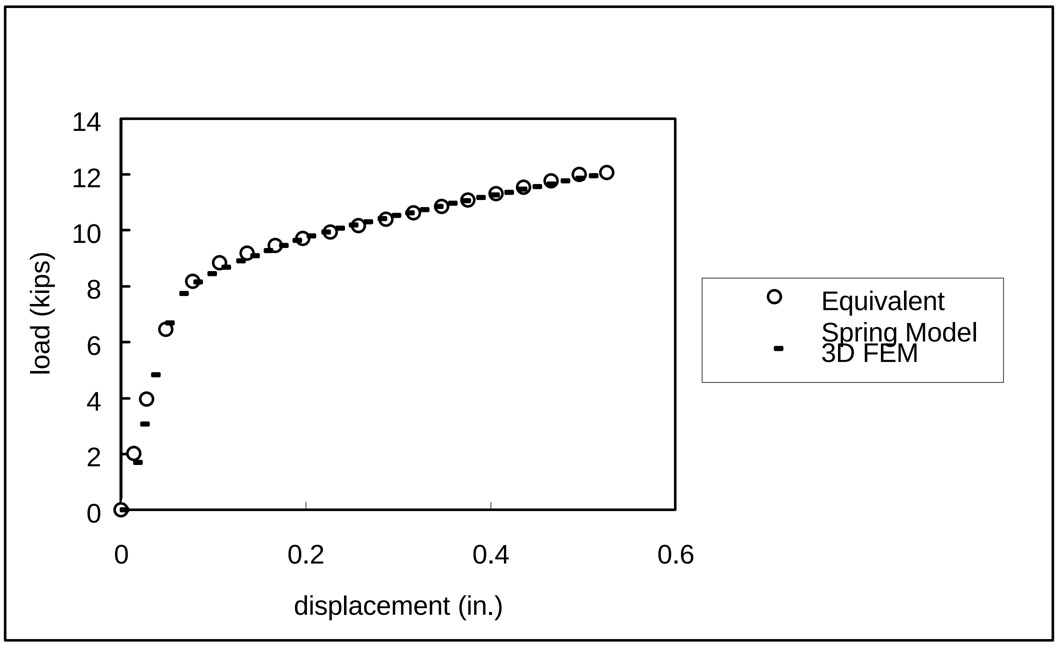

Figure 4.4 Load-Displacement Relationship for the L5x3x1/4 Double Angle Connection due to Tension Loading

Table 4.2 Data for the Load-Displacement Relationship of an L5x43x1/4 Double Angle

Connection due to Tension Loading

Loading Stage	Displacement (in.)	Load (kips)
1	0	0
2	0.0138	2
3	0.0276	3.945
4	0.0486	6.454
5	0.0777	8.169
6	0.107	8.824
7	0.137	9.175
8	0.167	9.445
9	0.197	9.691
10	0.227	9.927
11	0.257	10.16
12	0.287	10.39
13	0.317	10.62
14	0.347	10.85
15	0.376	11.07
16	0.406	11.3
17	0.436	11.53
18	0.466	11.76
19	0.496	11.98
20	0.526	12.07

Figure 4.5 presents the 3D FEM and simplified load-displacement relationships of the L5x3x3/8 double angle connection. The axial tensile load, *T*, varies from 0 kips to approximately 24 kips for this case. The axial tensile load, *T*, is applied to one end of the beam in the positive Z-direction. Like the previous L5x3x1/4 double angle connection, the load-displacement curve shows good agreement with that of the 3D finite element model from the beginning of the loading. The initial stiffness of the equivalent spring model is 554 kips/in., while that of the 3D finite element model is 477.5 kips/in. Table 4.3 presents the data for the load-displacement relationship of an L5x3x3/8 double angle connection.

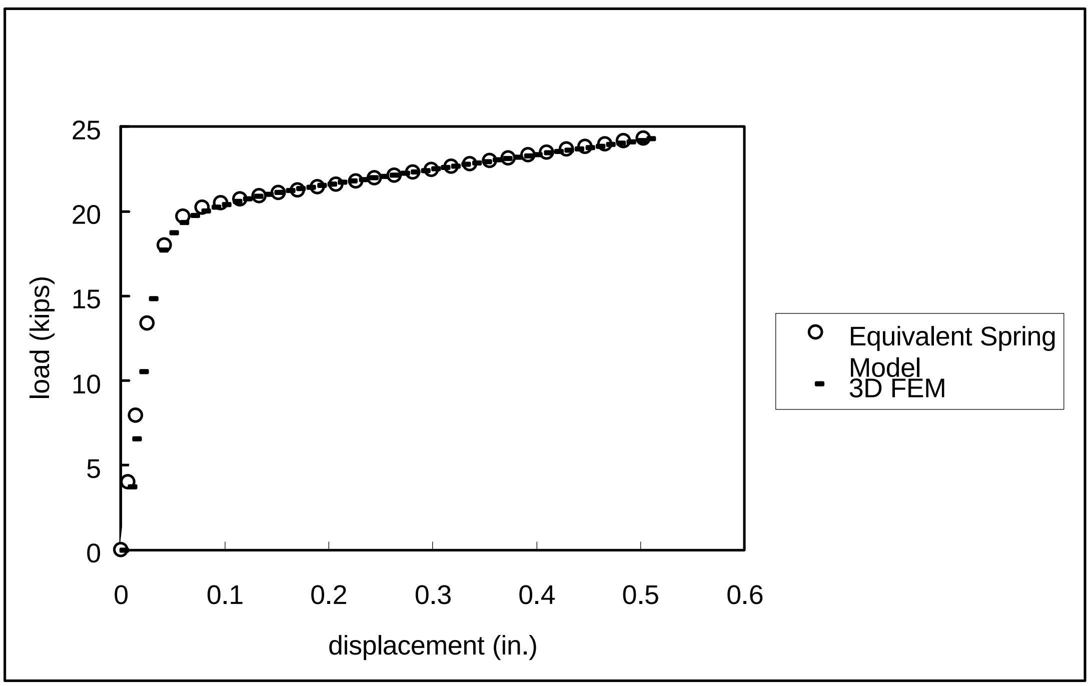

Figure 4.5 Load-Displacement Relationship for an L5x3x3/8 Double Angle Connection due to Tension Loading

Table 4.3 Data for the Load-Displacement Relationship of an L5x3x3/8 Double Angle Connection due to Tension Loading

Loading Stage	Displacement (in.)	Load (kips)
1	0	0
2	0.00722	4
3	0.0145	7.952
4	0.0256	13.37
5	0.042	18.01
6	0.0598	19.69
7	0.0781	20.23
8	0.0965	20.51
9	0.115	20.72
10	0.133	20.91
11	0.152	21.09
12	0.17	21.26
13	0.189	21.43
14	0.207	21.6
15	0.226	21.77
16	0.244	21.95
17	0.263	22.12
18	0.281	22.29
19	0.299	22.46
20	0.318	22.63
21	0.336	22.8
22	0.355	22.97
23	0.373	23.14
24	0.392	23.31
25	0.41	23.48
26	0.429	23.65
27	0.447	23.81
28	0.466	23.98
29	0.484	24.15
30	0.503	24.32

Figure 4.6 shows the load-displacement relationship of an L5x3x1/2 double angle connection. The axial tensile load, *T*, varies from 0 kips to approximately 39 kips for this case. The axial tensile load, *T*, is applied to one end of the beam in the positive Z-direction. Like the previous L5x3x1/4 double angle connection and L5x3x3/8 double

angle connection, the load-displacement curve shows good agreement with that of the 3D finite element model from the beginning of the loading. The initial stiffness of the equivalent spring model is 1,018.5 kips/in., while that of the 3D finite element model is 1,012.7 kips/in. Table 4.4 presents the data for the load-displacement relationship of an L5x3x1/2 double angle connection.

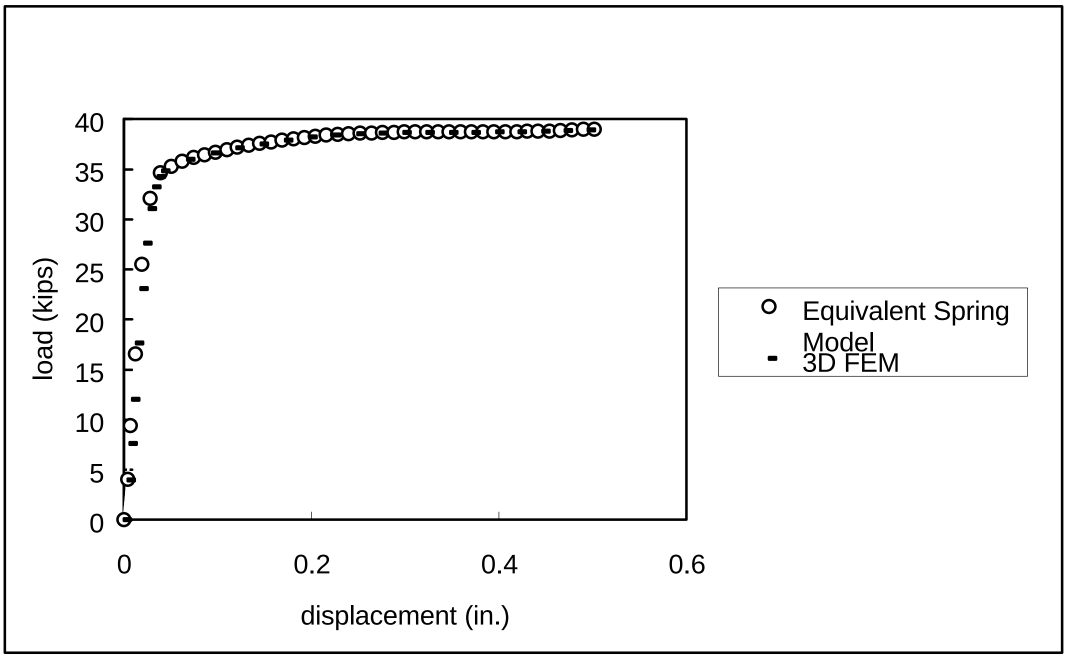

Figure 4.6 Load-Displacement Relationship of an L5x3x1/2 Double Angle Connection due to Tension Loading

Table 4.4 Data for the Load-Displacement Relationship of an L5x3x1/2 Double Angle Connection due to Tension Loading

Loading Stage	Displacement (in.)	Load (kips)
1	0	0
2	0.00394	4.013
3	0.00706	9.37
4	0.0123	16.55
5	0.0196	25.47
6	0.0284	32.06
7	0.0392	34.6
8	0.0508	35.24
9	0.0625	35.75
10	0.0743	36.13
11	0.086	36.42
12	0.0978	36.69
13	0.11	36.92
14	0.121	37.15
15	0.133	37.34
16	0.145	37.53
17	0.157	37.7
18	0.169	37.87
19	0.181	38.02
20	0.193	38.16
21	0.204	38.28
22	0.216	38.38
23	0.228	38.46
24	0.24	38.51
25	0.252	38.57
26	0.264	38.61
27	0.276	38.64
28	0.288	38.66
29	0.299	38.68
30	0.311	38.68
31	0.323	38.68
32	0.335	38.69
33	0.347	38.69
34	0.359	38.7
35	0.371	38.7
36	0.383	38.71
37	0.395	38.71
38	0.407	38.72
39	0.419	38.72
40	0.43	38.74

4.3.2 Equivalent Spring Model Under Shear Loading

The equivalent spring model is used in this section to establish the moment-rotation relationship of a double angle connection under shear loading. The moment-rotation relationship of an equivalent spring model can be obtained by determining the rotational angle change, θ, at z=0 along with the connection moment, *M*, at each loading stage. The connection moment, *M*, which is transferred to the supporting members, is defined as the moment developed at the corner of the angle due to the uniformly distributed load, *Q*. The rotational spring stiffness can be obtained from a regression analysis of the moment-rotation curve of the 3D finite element model.

Figure 4.7 shows the moment-rotation curves of the L5x3x1/4 double angle connection. The 3D FEM curve is in Figure 2.11 and the equivalent spring model is based on the Richard's formula parameters in Table 2.11. A uniformly distributed load, *Q*, has been applied to the beam of the equivalent spring model. Even though the moment-rotation curve shows an initial discrepancy with that of the 3D finite element model, it shows good agreement after some initial loading. The initial rotational spring stiffness of the equivalent spring model is 5,690 in.-kips/rad., while that of the 3D finite element model is approximately 3,560 in.-kips/rad. Table 4.5 contains the data for the moment-rotation relationship of an L5x3x1/4 double angle connection.

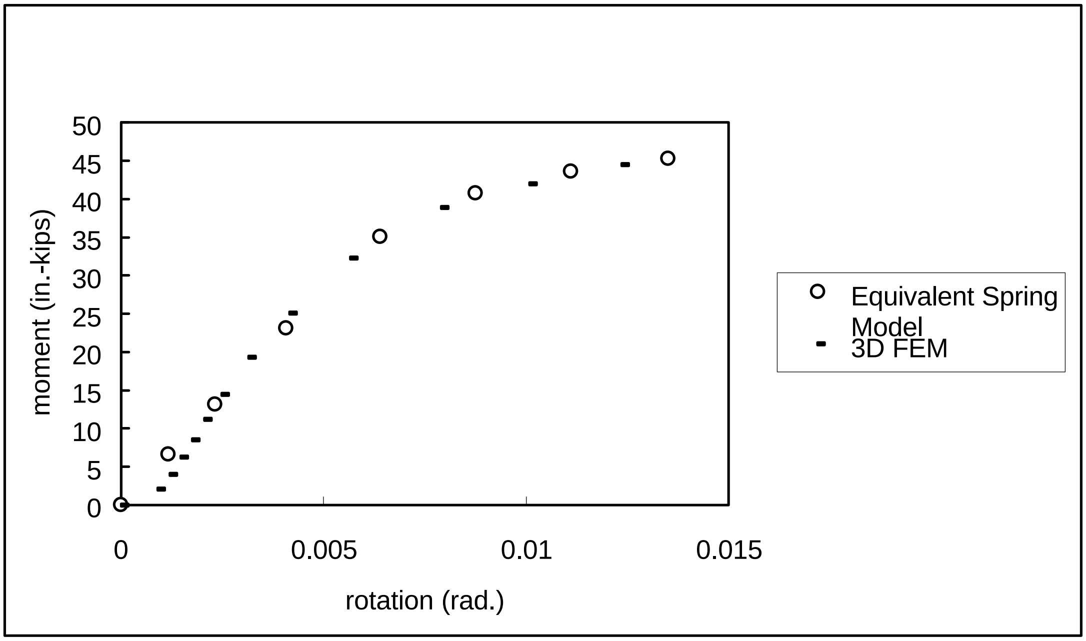

Figure 4.7 Moment-Rotation Relationship of an L5x3x1/4 Double Angle Connection due to Shear Loading

Table 4.5 Data for the Moment-Rotation Relationship of an L5x3x1/4 Double Angle Connection due to Shear Loading

Loading Stage	Applied Load (kips)	Rotation (rad.)	Moment (in.-kips)
1	0	0	0
2	4	0.00116	6.6
3	8	0.00232	13.2
4	14	0.00407	23.08
5	21.97	0.00639	35.08
6	29.82	0.00875	40.8
7	37.63	0.0111	43.65
8	45.4	0.0135	45.27

Figure 4.8 shows the moment-rotation relationship of an L5x3x3/8 double angle connection under the uniformly distributed load of 0.3334 kips/in. (total 80 kips). Like the previous L5x3x1/4 double angle connection, the moment-rotation relationship shows an initial discrepancy with that of the 3D finite element model. The initial rotational stiffness of the equivalent spring model is 20,455.5 in.-kips/rad., while that of the 3D finite element model is approximately 6,119 in.-kips/rad. Table 4.6 contains the data for the moment-rotation relationship of an L5x3x3/8 double angle connection.

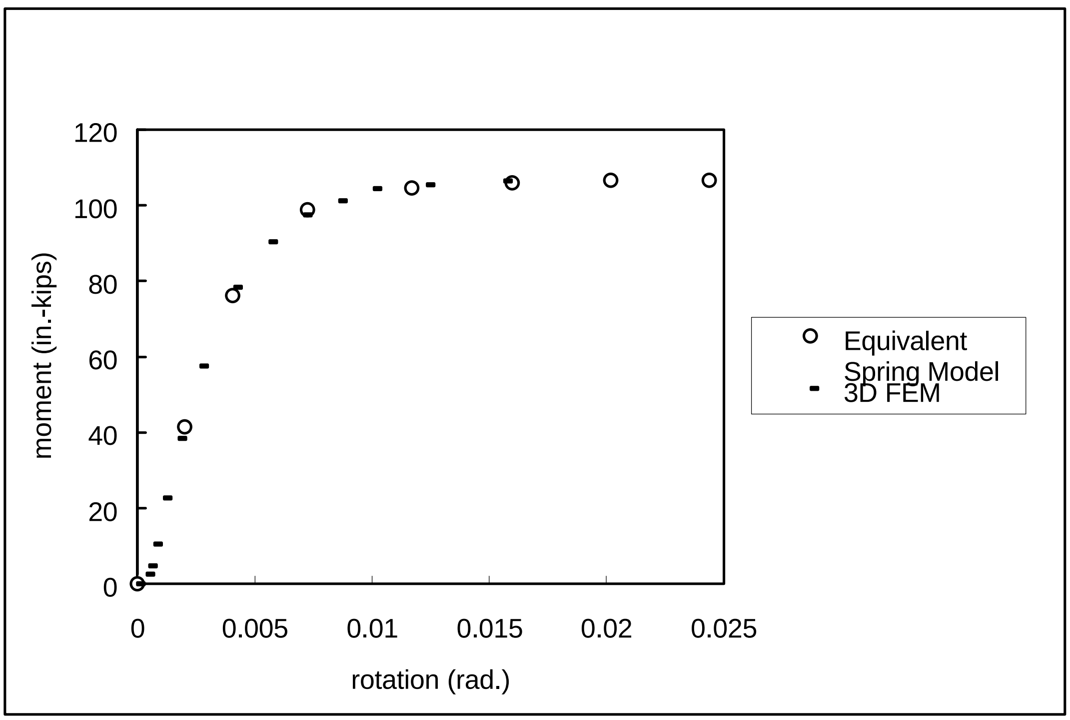

Figure 4.8 Moment-Rotation Relationship of an L5x3x3/8 Double Angle Connection due to Shear Loading

Table 4.6 Data for the Moment-Rotation Relationship of an L5x3x3/8 Double Angle Connection due to Shear Loading

Loading Stage	Applied Load (kips)	Rotation (rad.)	Moment (in.-kips)
1	0	0	0
2	7.99	0.00202	41.32
3	15.85	0.00406	76.11
4	27.05	0.00727	98.71
5	41.5	0.0117	104.4
6	55.15	0.016	105.9
7	64.3	0.0202	106.5
8	72.53	0.0244	106.5

Figure 4.9 shows the moment-rotation relationship of an L5x3x1/2 double angle connection. A uniformly distributed load of 0.3334 kips/in. (totally 80 kips) has been applied to the beam of the equivalent spring model. Like the previous two cases, the moment-rotation relationship of the equivalent spring model shows an initial discrepancy with that of the 3D finite element model. The initial rotational stiffness of the equivalent spring model is 49,213 in.-kips/rad., while that of the 3D finite element model is approximately 14,606 in.-kips/rad. Table 4.7 contains the data for the moment-rotation relationship of an L5x3x1/2 double angle connection.

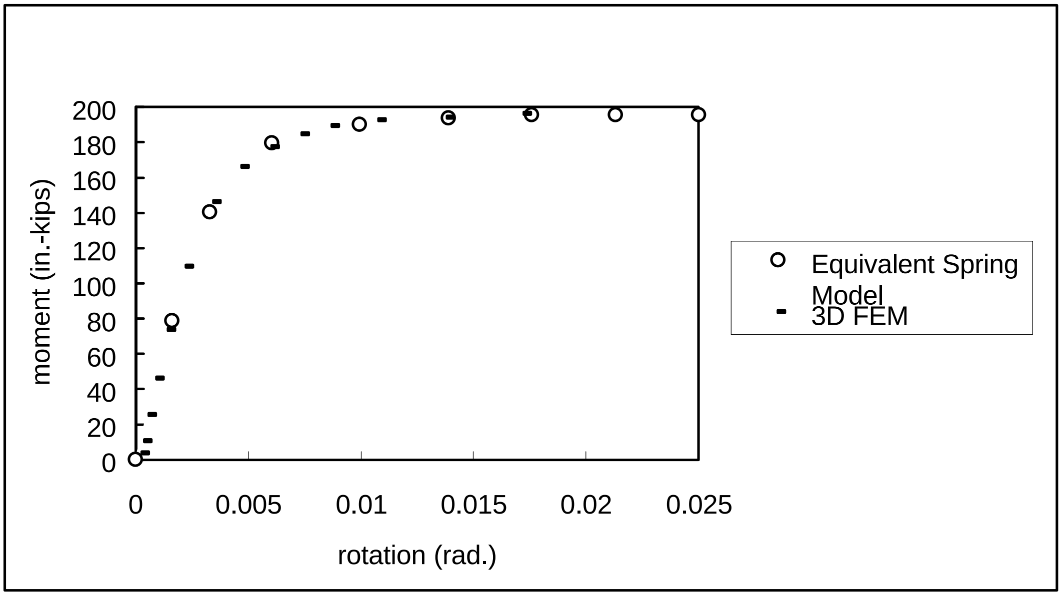

Figure 4.9 Moment-Rotation Relationship of an L5x3x1/2 Double Angle Connection due to Shear Loading

Table 4.7 Data for the Moment-Rotation Relationship of an L5x3x1/2 Double Angle Connection due to Shear Loading

Loading Stage	Applied Load (kips)	Rotation (rad.)	Moment (in.-kips)
1	0	0	0
2	7.967	0.0016	78.74
3	15.597	0.00329	140.6
4	25.956	0.00606	179.6
5	38.934	0.00994	190.1
6	51.765	0.0139	193.8
7	61.446	0.0176	195.7
8	69.09	0.0213	195.7
9	76.272	0.025	195.7

4.4 DISCUSSION OF THE RESULTS OF THE SIMPLIFIED MODELS

Under applied tensile loads, the initial stiffness of the L5x3x1/4 3D finite element angle model is 116.7 kips/in., while that of the simplified angle model is 124.2 kips/in. from the previous section. The simplified angle model shows a higher initial stiffness than that of the 3D finite element model by 6.03 %. For the L5x3x3/8 finite element angle model, the initial stiffness is 477.5 kips/in., while that of the simplified angle model is 442.6 kips/in. The 3D finite element model shows a higher initial stiffness than that of the simplified angle model by 7.32 % in this case. Similarly, the initial stiffness of the L5x3x1/2 finite element angle model is 1,012 kips/in., while that of the simplified angle model is 1,109 kips/in. The simplified angle model shows a higher initial stiffness than that of the 3D finite element model by 9.5 %. Considering these results, the initial stiffness of the simplified angle model gives good agreement with that of the 3D finite element model under axial tensile loads. Thus, this simplified angle model can be useful for initial design of a double angle connection under axial tensile loads.

Considering the behavior of each double angle connection under axial tensile loads, the suggested equivalent spring gives good results for each case from the beginning of the loading. Each angle specimen considered in this research has the same material properties and geometrical properties except for the angle thickness, t. The thicknesses of the angles used for this research are 1/4 in., 3/8 in., and 1/2 in., respectively. Table 4.8 contains the data for the main parameters used in Richard's formula for the load-displacement curve of the equivalent spring model. Using Richard's formula in Section 2.4.1, each parameter can be obtained from a regression analysis of the load-displacement curve.

Table 4.8 Data for the Main Parameters used in Richard's Formula for the Equivalent Spring Model under Tension Loading

	K (*kips/in.*)	*K*p (*kips/in.*)	*R*o (*kips*)	*n*
L5x3x1/4 Angle	145.3	7.5	8.3	3.8
L5x3x3/8 Angle	551.3	9.2	19.7	4.0
L5x3x1/2 Angle	1381.5	5.2	36.8	3.6

From the above table, the increase of initial stiffness, *K*, is approximately proportional to $(t/b)^3$, while that of the reference load, R_0, is approximately proportional to $(t/b)^2$ for each case.

The equivalent spring model also shows good agreement for the moment-rotation relationship with the results of the 3D finite element analysis at the beginning of loading. The same angle properties as above are used for the analysis of the moment-rotation relationships. Table 4.9 shows the data for the main parameters used in Richard's formula for the moment-rotation curves. Like the previous cases, the increase of initial rotational stiffness, *K*, is approximately proportional to $(t/b)^3$, while that of the reference moment, R_0, is approximately proportional to $(t/b)^2$ for each case. The values of the curve sharpness parameter, n, are equal to 7.7, 3.6, and 2.9, respectively.

Table 4.9 Data for the Main Parameters used in Richard's Formula for the Equivalent Spring Model under Shear Loading

	K (*in.-kips/rad.*)	*K*p (*in.-kips/rad.*)	*R*o (*in.-kips*)	*n*
L5x3x1/4 Angle	5,694.7	754.4	35.2	7.7
L5x3x3/8 Angle	20,698	66.3	105.2	3.6
L5x3x1/2 Angle	50,540	109.4	193.7	2.9

4.5 SUMMARY AND CONCLUSIONS

Considering the results of the equivalent spring model, this model can be a good substitution for the more complex 3D nonlinear finite element model under axial tensile loads. Even though the results of the equivalent spring model show a little discrepancy with those of the 3D nonlinear finite element model under shear loads, it can also be a good starting point for the investigation of the actual double angle connection behavior.

Thus, this equivalent spring model satisfies the needs for saving the cost and the time of the computer required for a full 3D analysis of the double angle connection.